Fiber reinforced shape-memory polymer composite and its application in a deployable hinge

2009 Smart Mater. Struct. 18 024002

(http://iopscience.iop.org/0964-1726/18/2/024002)

Smart Mater. Struct. **18** (2009) 024002 (6pp) doi:10.1088/0964-1726/18/2/024002

Fiber reinforced shape-memory polymer composite and its application in a deployable hinge

Xin Lan[1], Yanju Liu[2], Haibao Lv[1], Xiaohua Wang[1], Jinsong Leng[1] and Shanyi Du[1]

[1] Center for Composite Materials and Structures, Harbin Institute of Technology, People's Republic of China
[2] Department of Aerospace Science and Mechanics, Harbin Institute of Technology, People's Republic of China

E-mail: yj_liu@hit.edu.cn

Received 14 May 2008, in final form 10 August 2008
Published 20 January 2009
Online at stacks.iop.org/SMS/18/024002

Abstract

This paper investigates the shape recovery behavior of thermoset styrene-based shape-memory polymer composite (SMPC) reinforced by carbon fiber fabrics, and demonstrates the feasibility of using an SMPC hinge as a deployable structure. The major advantages of shape-memory polymers (SMPs) are their extremely high recovery strain, low density and low cost. However, relatively low modulus and low strength are their intrinsic drawbacks. A fiber reinforced SMPC which may overcome the above-mentioned disadvantages is studied here. The investigation was conducted by three types of test, namely dynamic mechanical analysis (DMA), a shape recovery test, and optical microscopic observations of the deformation mechanism for an SMPC specimen. Results reveal that the SMPC exhibits a higher storage modulus than that of a pure SMP. At/above T_g, the shape recovery ratio of the SMPC upon bending is above 90%. The shape recovery properties of the SMPC become relatively stable after some packaging/deployment cycles. Additionally, fiber microbuckling is the primary mechanism for obtaining a large strain in the bending of the SMPC. Moreover, an SMPC hinge has been fabricated, and a prototype of a solar array actuated by the SMPC hinge has been successfully deployed.

(Some figures in this article are in colour only in the electronic version)

1. Introduction

Smart materials have attracted much interest in recent years. Their applications cover non-destructive evaluation [1], dynamics control [2], and shape control, etc. Shape memory polymers (SMPs) are one candidate actuation material in the field of shape control. They are able to recover their original shape upon applying an external stimulus [3, 4], such as heat [5, 6], light [7], and moisture [8–10]. Among these SMPs, the thermo-responsive SMP is common. As shown as figure 1, the general thermomechanical cycle of a thermo-responsive SMP consists of the following steps [11, 12]. (1) Fabricate the SMP into a shape (original shape); (2) heat and deform the SMP above T_g by applying an external force, cool well below T_g, remove the constraint and then get the temporary pre-deformed shape (storage); (3) heat the pre-deformed SMP above T_g, and then the SMP recovers towards the original shape (recovery).

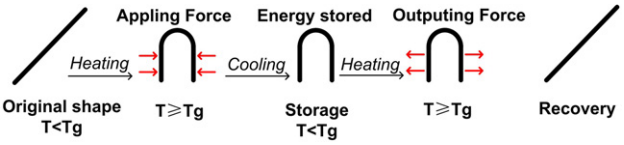

Figure 1. Schematic of the shape-memory effect during typical thermomechanical cycles.

An SMP shows very good shape recoverability, easy shaping procedure, low density and cost, and easy control

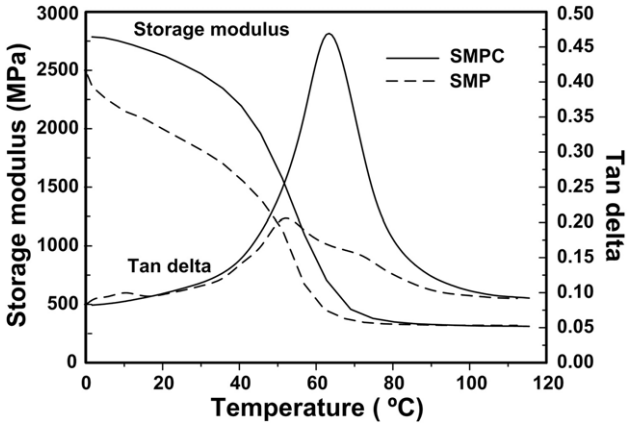

Figure 2. Storage modulus and tangent delta versus temperature of the pure SMP and SMPC.

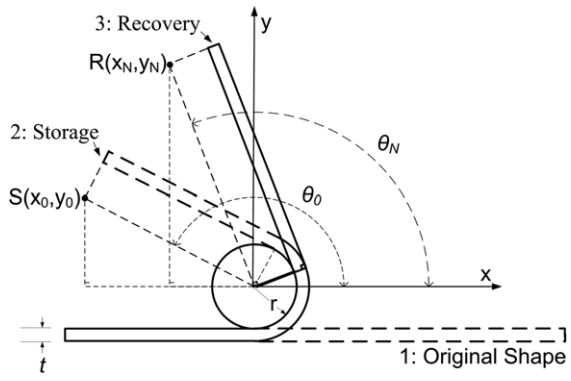

Figure 3. Schematic illustration of the setup for the shape recovery performance test.

of the recovery temperature [3, 4]. However, pure SMPs are not suitable for many practical applications that require particular functions (e.g., high strength, high recovery force, and good electrical conductivity). Therefore, shape-memory polymer composites (SMPCs) filled with particles (e.g., carbon black [13–15], carbon nanotubes [16, 17], Ni [18, 19], Fe_3O_4 [20], SiC [21], short fibers or continuous fibers [22–25]) have been studied to meet the various requirements in practical applications. In general, an SMPC filled with particles or short fibers develops some particular functions, such as electrical conductivity [13–19], magnetic-responsive performances [20], and high stiffness in the micro scale [21]. However, the improvement in mechanical properties is quite limited [13–21], so an SMPC filled with particles or short fibers could not be used as a structural material due to the low strength and stiffness. By contrast, a continuous-fiber reinforced SMPC represents excellent mechanical properties [22–25]. As both a functional and structural material, continuous-fiber reinforced SMPC shows good potential in many advanced applications. When a fiber reinforced SMPC is used as an actuator material, there are no moving parts. Therefore, this type of SMPC has caused substantial interest in deployable structures such as deployable antennae, trusses and solar arrays in the space industry and other applications.

In this paper, a new type of fiber reinforced thermoset styrene-based shape-memory polymer composite (SMPC) is developed. The main objective is to systematically characterize the shape recovery properties of the SMPC, which is a foundation for SMPCs used in deployable structures. Our focuses include the basic mechanical performances, shape recovery performances, microstructural deformation mechanisms and its application in a deployable hinge.

2. Experimental methods

The polymer matrix used in the current study is a thermoset styrene-based SMP resin (CRG Industries, Veriflex®). The SMP resin includes two parts: resin and curing agent. When curing, the resin and curing agent is mixed in the weight ratio 28:1. The SMPC specimen and SMPC hinge are reinforced by T300 carbon fiber plain-weave fabrics. The composite is fabricated by the standard fabrication techniques for fiber reinforced composite: curing of a preimpregnated fabric. The SMPC was reinforced by three-ply plain weaves. It was cured at 75 °C for 48 h, under a pressure of 0.7 MPa. When cured, the thickness of the SMPC specimen is around 3 mm. For comparison, a pure SMP specimen was cured under the same conditions as those for the SMPC.

In order to investigate the basic performances of the pure SMP and SMPC at different temperatures, a dynamic mechanical analyzer (DMA: NETZSCH, DMA242C) was used to determine the storage modulus and tangent delta. Three-point bending mode was applied with a span of 40 mm. The dimensions of the specimens were 50 mm × 9 mm × 3 mm. The scanning range of temperature was 0–120 °C at a heating rate of 2 °C min^{-1} and a frequency of 1 Hz. Moreover, in order to investigate the shape recovery performances of the SMPC, a shape recovery test upon bending of the SMPC specimen was performed in a water bath. In addition, to determine the microstructural mechanisms of the SMPC under bending deformation, an optical microscope (ZEISS MC80DX) was used to observe the microstructural deformation after the shape recovery tests. Finally, a hinge made of SMPC was manufactured, and then we performed a deployment experiment of a prototype of a solar array actuated by the SMPC hinge.

3. Experimental results and discussions

3.1. Dynamic mechanical analysis

The DMA test shows storage modulus and tangent delta versus temperature for the pure SMP and SMPC (figure 2). According to the curves of storage modulus, it is clear that the SMPC has a higher storage modulus than that of pure SMP within the range of 0–80 °C. The storage modulus of the SMPC falls apparently within the glass transition region of about 40–80 °C, namely $T_g - 20$ °C to $T_g + 20$ °C. The peak value of tangent delta is defined as T_g. Hence, the T_g value of the pure SMP and SMPC is found to be about 54 °C and 64 °C, respectively.

3.2. Shape recovery performance

For practical application of the SMPC, its shape recovery performance is extremely important. Therefore, a systematic

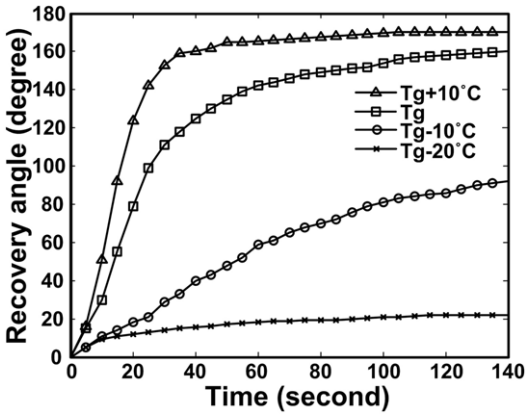

Figure 4. Recovery angle versus time during the shape recovery process at different ambient temperatures ($T_g - 20\,°C$, $T_g - 10\,°C$, T_g, $T_g + 10\,°C$, where T_g is about 64 °C).

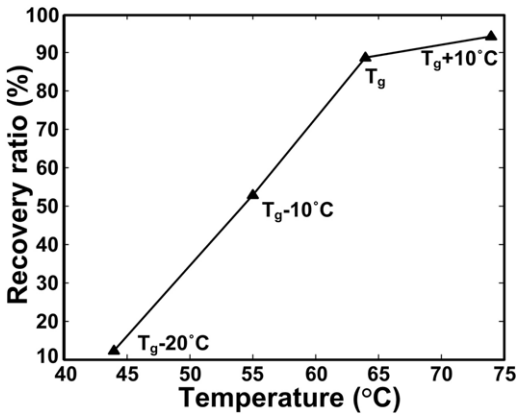

Figure 5. Shape recovery ratio at different ambient temperatures. The original storage angle θ_0 is 180° in the storage state; the residual angle θ_1 in the recovery state is selected at the 140th second during the first shape recovery cycle.

shape recovery test of SMPC specimens upon bending was performed. The procedure for the thermomechanical bending cycling of the SMPC includes the following steps (see figure 3): (1) the specimen in its original shape is kept in a water bath for 5 min at $T_g + 20\,°C$; (2) the SMPC is bent to a storage angle θ_0 around a mandrel with the radius of 2 mm in the soft rubbery state, and then the SMPC is kept in cool water with the external constraint to 'freeze' the elastic deformation energy for 5 min (storage); (3) the SMPC specimen fixed on the apparatus is immersed into another water bath at an elevated temperature, and then it recovers to an angle θ_N (recovery). The method used to quantify the precision of deployment is illustrated in figure 3, where r denotes the radius of the mandrel, t represents the thickness of the SMPC specimen, θ_0 is the original storage angle of the specimen in the storage state during the first bending cycle, and $S(x_0, y_0)$ is a point selected to determine θ_0. θ_N is the residual angle in the recovery state during the Nth thermomechanical bending cycle ($N = 1, 2, 3, \ldots$). $R(x_N, y_N)$ is a testing point in order to calculate θ_N:

$$\theta_N = \mathrm{ArcCot}\left(\frac{x_N}{y_N}\right) \quad (N = 1, 2, 3, \ldots, \quad 0 \leqslant \theta_N \leqslant 180^\circ). \tag{1}$$

The value of the shape recovery ratio is calculated by

$$R_N = \frac{\theta_0 - \theta_N}{\theta_0} \times 100\% \qquad (N = 1, 2, 3, \ldots), \tag{2}$$

where R_N denotes the shape recovery ratio of the Nth thermomechanical bending cycle. $S(x_0, y_0)$ and $R(x_N, y_N)$ are measured by a vernier caliper with a resolution of 0.01 mm. Finally, θ_N and R_N are obtained through equations (1) and (2). In the following tests, the radius r of the mandrel and thickness t of SMPC specimen are 2 mm and 3 mm, respectively.

3.2.1. Shape recovery performance at various ambient temperatures. In order to investigate the shape recovery velocity and shape recovery ratio R_1 of the SMPC at different temperatures, testing of the recovery angle versus time was conducted at different temperatures, namely $T_g - 20\,°C$, $T_g - 10\,°C$, T_g, $T_g + 10\,°C$. The pre-deformed temperature of the SMPC was set as T_g of the SMPC (64 °C). The original storage angle θ_0 was selected as 180°.

Figure 4 shows the relationship between recovery angle and time of four different SMPC specimens at various ambient temperatures. At/above the temperature T_g, associated with a fast glass transition and strain energy dissipation of the SMP, the SMPC specimens deploy quickly within the initial 30 s, and then the deployment velocity drop quickly due to the termination of energy dissipation. Below T_g, the SMPC specimens deploy very slowly due to the partial glass transition and energy dissipation of the SMP. In addition, based on figure 4, a shape recovery ratio R_1 is defined (see figure 5) where the residual angle θ_1 is selected at the 140th second in the first deformation cycle ($N = 1$). As shown in figure 5, at/above the temperature T_g, the shape recovery ratio remains relatively stable, which corresponds to the full glass transition above T_g of the SMP. Moreover, the shape recovery behavior can also be observed within the range of $T_g - 20\,°C$ and T_g, which is associated with the partial glass transition (see figure 2). However, the shape recovery ratio drops sharply when the ambient temperature decreases to $T_g - 20\,°C$. The shape recovery effect cannot be released below an ambient temperature of $T_g - 20\,°C$.

3.2.2. Shape recovery ratio upon bending cycling. In order to evaluate the degradation of deployment, the shape recovery ratio R_N corresponding to the number of bending cycles N was tested at a original bending angle $\theta_0 = 180°$ at $T_g + 20\,°C$ (see figure 6). It shows that the recovery ratio R_N decreases from 96% to 91% during the first 50 bending cycles. The shape recovery ratio becomes relatively stable after the 30th bending cycle, and remains at approximately 90%. In addition, for the deployment process, the SMPC deployed within approximately 2 min; the recovery velocity in the first 30 s is relatively high (see figure 4).

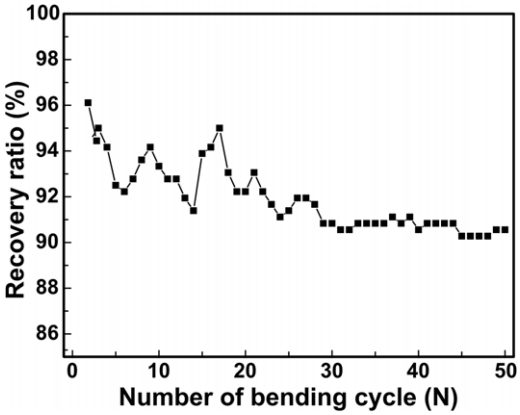

Figure 6. Shape recovery ratio versus the number of bending cycles at $T_g + 20\,^{\circ}\mathrm{C}$.

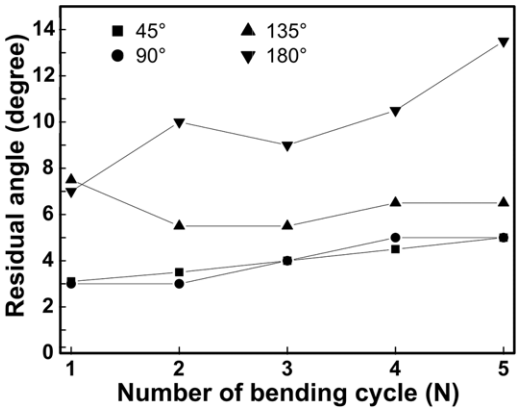

Figure 7. Residual angle θ_N ($N = 1, 2, 3, 4, 5$) versus the number of bending cycles at different original storage angles θ_0 (45°, 90°, 135°, 180°).

3.2.3. Residual angles under the condition of different original storage angles. As the storage deformation of SMPC structures may be of various types, a characterization of the shape recovery performances at different bending angles θ_0 was performed. The relationship of residual angle θ_N ($N = 1, 2, 3, 4, 5$) and original storage angles θ_0 ($\theta_0 =$ 45°, 90°, 135° and 180°) was investigated (figure 7). Results indicate that the residual angle of the SMPC corresponding to the original bending angle of 45° is the lowest (3°–5°). The SMPC laminate with larger storage angle θ_0 results in a larger residual angle θ_N.

In conclusion, the shape recovery ratio under bending is high at/above T_g, while the shape-memory effect can also be observed below T_g but still within the region of the glass transition, although the shape recovery ratio is low. The stability of the shape recovery properties of the SMPC depends strongly on the number of thermomechanical cycles. Upon bending cycling, the total instant reversible strain deteriorates, and becomes relatively stable after sufficient numbers of packaging/deployment cycles, which contributes to the training effect of the materials.

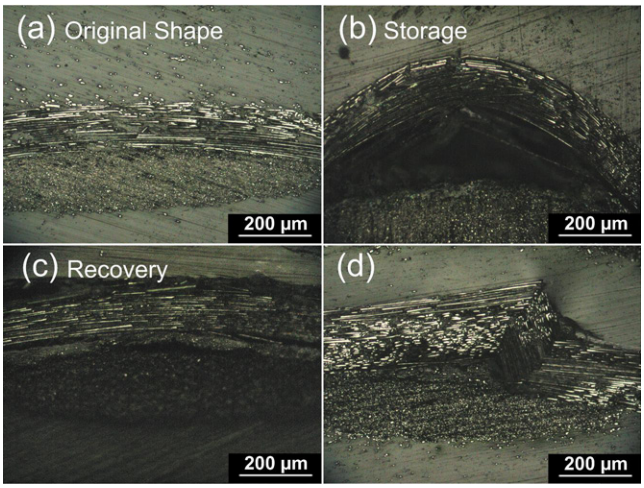

Figure 8. Optical microscopic images of microstructures of SMPC specimens. SMPC specimen after 50 bending cycles in different shapes: (a) the original shape before bending, (b) the storage shape with an original bending angle $\theta_0 = 180°$, and (c) the recovery shape. (d) SMPC specimen upon bending after a static three-point bending test at room temperature.

3.3. Microscopic observation of the microstructural deformation mechanism in the shape recovery process

During the macroscopic shape recovery process, the shape recovery performance of the SMPC is determined not only by the shape-memory effect of the SMP but also by the microstructural deformation mechanism of the fiber and the SMP. Hence, a microscopic observation was conducted for the SMPC specimen during the shape recovery process. As is well known, the tensile stiffness of carbon fiber is much higher than its compressive stiffness and the stiffness of the SMP matrix. Thus, we assume that, upon applying a bending force on the SMPC specimen, the neutral axis of the bent specimen moves from the middle plane towards the outer surface where the fibers are in a tensile stress state. As a result, all the other fibers except for those on the outer surface are in the compressive stress state [23]. Consequently, the traditional assumptions in simple beam theory can be applied here. Based on the assumption of the linear distribution of the compressive strains along the thickness of the specimen, one has

$$\frac{r}{t} = \frac{1}{\varepsilon} \tag{3}$$

where r denotes the radius of the mandrel, t represents the thickness of the specimen (see figure 3) and ε is the maximum strain on the inner surface.

The microstructure, particularly with respect to the fiber microbuckling of the specimen, was observed with an optical microscope when 50 thermomechanical cycles were finished. In addition, the traditional fiber reinforced laminate can be bent to an r/t value on the order of 100 ($\varepsilon \approx 1\%$), while the SMPC laminate in this study was bent to extremely large deformation with a small r/t value (0.667) to evaluate the shape recovery performances and observe fiber microbuckling. We aim to investigate the microstructural mechanism of

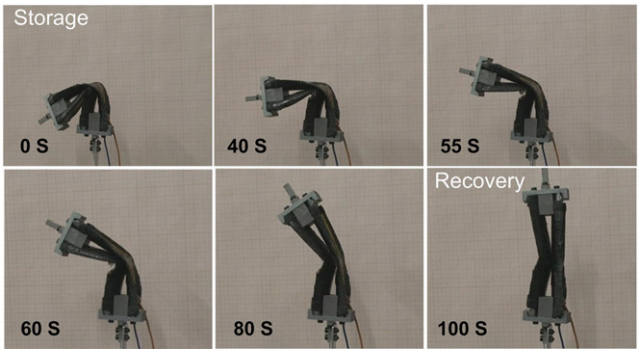

Figure 9. Shape recovery process of the SMPC hinge.

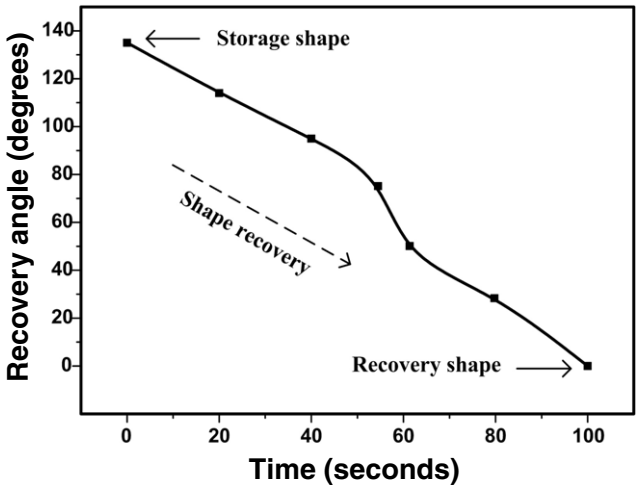

Figure 10. Relationship of recovery angle and time during the shape recovery process of the SMPC hinge.

SMPC specimens under large deformation upon bending in the thermomechanical cycles (see figure 3). The microstructure of the SMPC specimens was observed in three shapes after 50 thermomechanical cycles ($N = 50$), namely the original shape before bending (figure 8(a)), the storage shape with the original storage angle $\theta_0 = 180°$ (figure 8(b)), and the recovery shape $\theta_{50} \approx 16°$ (figure 8(c)). In addition, for comparison, we investigated the microstructure of an SMPC specimen upon bending after a static three-point bending test at room temperature (figure 8(d)).

Figure 8(a) shows an optical microscopic image of an SMPC specimen in a side-view right after fabrication without deformation. Before applying the bending force, the bonding among transverse fibers, longitudinal fibers and the SMP matrix is pretty good, namely there is no failure or delamination in the composite. Figure 8(b) reveals fiber microbuckling at the original storage angle $\theta_0 = 180°$. A large delamination gap can be observed between the transverse fiber tow and the longitudinal fiber tow. The sine shape of microbuckling of the transverse fiber tow can also be observed. Figure 8(c) shows the recovered configuration of fiber microbuckling at the same location as figure 8(b). A small recovered delaminate gap can also be observed between the transverse fiber tow and the longitudinal fiber tow. Figure 8(d) presents the buckled fracture of the transverse fiber tow after a static three-point bending test at room temperature ($T_g - 40\,°C$). It is clear that the buckling fracture of transverse fiber tow occurs on the inner surface beyond the compressive strain limit of the fiber.

In the thermomechanical cycle of pre-deformation and shape recovery stage ($T \geqslant T_g$), the stiffness of the SMP matrix was low enough to provide mobility for fibers to avoid the extreme local strain/stress and permanent fiber buckling failure. Due to the microbuckling of the fiber and the SMP, only fiber microbuckling but no fiber fracture was observed during the thermomechanical cycles. In addition, based on equation (3), the maximum theoretical strain on the inner surface of the bent SMPC specimen is calculated as $\varepsilon = 150\%$, where the thickness t of the specimen and radius r of mandrel are 3 mm and 2 mm, respectively. As is well known, the strain limit ε_{limit} of carbon fiber is 0.5–1%. Therefore, it is obvious that the SMPC specimen achieves a much higher strain than the strain limit of the carbon fiber associated with the microbuckling of the fiber and the SMP. By contrast, at $T \leqslant T_g - 40\,°C$, due to the relatively high stiffness of the SMP matrix, the mobility of the buckled fiber in the high compressive strain state is limited by the strong constraint of the SMP matrix, which leads to a brittle fracture of the transverse fiber. Consequently, both fiber fracture and microbuckling were observed in the static three-point bending test at room temperature.

SMPC materials are similar to traditional fiber reinforced composites except for the use of a thermoset styrene-based shape-memory resin that enables much higher packaging strains than traditional composites without damage to the fibers or the resin. This high strain capacity can lead to SMPC component designs that can be packaged more compactly than designs made with other materials. In order to achieve high package strain and avoid fiber failure in the storage state, fiber microbuckling is needed. With microbuckling, SMPC materials are suited for use in deployable space structure components because of their high strain-to-failure capability [23–25]. It should also be noticed that buckling and delamination in composites will unavoidably reduce the mechanical properties of SMPCs, which will be discussed in detail in our future study.

3.4. SMPC hinge

Using the SMPC, we designed an SMPC hinge, and then actuated a prototype of a solar array using this SMPC hinge. The SMPC hinge consists of two curved circular SMPC shells. The length of each curved SMPC laminate is 100 mm. The radius of the circular SMPC laminate is 12.5 mm, with a thickness of 3 mm. The weight is 14.5 g for each piece of SMPC laminate. Figure 9 shows the deployment process of the SMPC hinge. An voltage of 20 V is applied on the embedded resistor heater in each circular laminate with a current of about 0.8 A. Hence, the total power of the hinge with two circular laminates is about 32 W. The temperature of the SMPC hinge remains at about 80 °C after heating for 30 s. The original

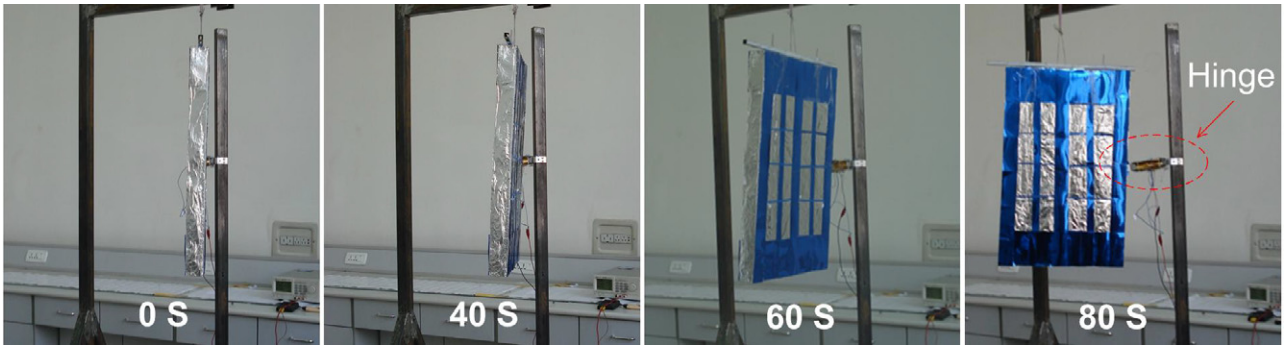

Figure 11. Shape recovery process of a prototype of a solar array actuated by an SMPC hinge.

storage angle of the SMPC hinge in storage state is about 140°. The whole deployment process takes about 100 s. As shown in figure 10, the deployment velocity of the hinge in the medium stage is relatively higher than those in the initial and final stages. The deployment ratio approaches approximately 100%.

Figure 11 shows a deployment process of a prototype of a solar array which is actuated by an SMPC hinge. Heated by a voltage of 20 V, the SMPC hinge was bent to a original storage angle 90° upon applying an external force at a relatively soft state above T_g of the SMPC. After fixing the storage shape at room temperature, the SMPC hinge was heated again by applying the same voltage. The prototype of the solar array, actuated by the SMPC hinge, deployed from 90° to ∼0° in approximately 80 s.

4. Conclusions

In this paper, the performance of a carbon fiber fabric reinforced composite based on a styrene-based SMP is investigated. It may be concluded that: (1) the SMPC presents a higher storage modulus than those of pure SMPs; (2) the shape recovery ratio of the SMPC is above 90% at/above T_g, while it drops sharply below T_g. The shape recovery properties of the SMPC depend strongly on the number of thermomechanical cycles, and they become relatively stable after some packaging/deployment cycles; (3) microbuckling is the primary mechanism in the bending deformation of SMPC, which provides a higher bending strain than that in a traditional structural composite; (4) a hinge made of the SMPC can be fabricated, and a full shape recovery can be achieved in about 2 min. Moreover, a prototype of a solar array actuated by such an SMPC hinge deploys successfully in 80 s.

References

[1] Leng J S and Asundi A 2002 *NDE & E Int.* **35** 1
[2] Leng J S and Asundi A 1999 *Smart Mater. Struct.* **8** 256
[3] Behl M and Lendlein A 2007 *Mater. Today* **10** 20
[4] Ratna D and Karger-Kocsis J 2008 *J. Mater. Sci.* **43** 254
[5] Liu Y P, Gall K, Dunn M L and Cluskey P M 2004 *Mech. Mater.* **36** 929
[6] Ji F, Zhu Y, Hu J, Liu Y, Yeung L and Ye G 2006 *Smart Mater. Struct.* **15** 1547
[7] Lendlein A, Jiang H Y, Junger O and Langer R 2005 *Nature* **434** 879
[8] Huang W M, Yang B, An L, Li C and Chan Y S 2005 *Appl. Phys. Lett.* **86** 114105
[9] Leng J S, Lv H B, Liu Y J and Du S Y 2008 Comment on 'Water-driven programmable polyurethane shape memory polymer: demonstration and mechanism' [Appl. Phys. Lett. 86, 114105, (2005)] *Appl. Phys. Lett.* **92** 206105
[10] Leng J S, Lv H B, Liu Y J and Du S Y 2008 Shape-memory polymer in response to solution *Adv. Eng. Mater.* **10** 6
[11] Tobushi H, Okumura K, Hayashi S and Ito N 2001 *Mech. Mater.* **33** 545
[12] Liu C, Chun S B and Mather P T 2002 *Macromolecules* **35** 9868
[13] Yang B, Huang W M, Li C and Chor J H 2005 *Scr. Mater.* **53** 105
[14] Yang B, Huang W M, Li C and Li L 2006 *Polymer* **47** 1348
[15] Leng J S, Lv H B, Liu Y J and Du S Y 2007 *Appl. Phys. Lett.* **91** 144105
[16] Cho J W, Kim J W, Jung Y C and Goo N S 2005 *Rapid Commun.* **26** 412
[17] Sahoo N G, Jung Y C, Yoo H J and Cho J W 2007 *Compos. Sci. Technol.* **67** 1920
[18] Leng J S, Huang W M, Lan X, Liu Y J, Liu N, Phee S J, Yuan Q and Du S Y 2008 *Appl. Phys. Lett.* **92** 014104
[19] Leng J S, Huang W M, Lan X, Liu Y J and Du S Y 2008 Significantly reducing electrical resistivity by forming conductive Ni chains in a polyurethane shape-memory polymer/carbon-black composite *Appl. Phys. Lett.* **92** 204101
[20] Schmidt A M 2006 *Rapid Commun.* **27** 1168
[21] Gall K and Dunn M L 2002 *Acta Mater.* **50** 5115
[22] Zhang C S and Ni Q Q 2007 *Compos. Struct.* **78** 153
[23] Gall K, Mikulas M and Munshi N A 2000 *J. Intell. Mater. Syst. Struct.* **11** 877
[24] Abrahamson E R, Lake M S, Munshi N A and Gall K 2003 *J. Intell. Mater. Syst. Struct.* **14** 623
[25] Schultz M R, Francis W H, Campbell D and Lake S M 2007 *AIAA 2007-2401: 48th AIAA/ASME/ASCE/AHS/ASC Structures, Structural Dynamics, and Materials Conf. (Honolulu, Hawaii, April)*